

## The Interpretation of Electron Diffraction Patterns from Hydrocarbon Films

J. Karle and L. O. Brockway

Citation: [The Journal of Chemical Physics](#) **15**, 213 (1947); doi: 10.1063/1.1746482

View online: <http://dx.doi.org/10.1063/1.1746482>

View Table of Contents: <http://scitation.aip.org/content/aip/journal/jcp/15/5?ver=pdfcov>

Published by the [AIP Publishing](#)

---

### Articles you may be interested in

[Diffraction-modified Kerr rotation from patterned garnet films](#)

J. Appl. Phys. **107**, 09A923 (2010); 10.1063/1.3367969

[Computation of electron diffraction patterns in Lorentz electron microscopy of thin magnetic films](#)

J. Appl. Phys. **69**, 2455 (1991); 10.1063/1.348682

[The Scattering of Electrons by Hydrocarbon Films](#)

J. Chem. Phys. **14**, 297 (1946); 10.1063/1.1724137

[Geometric Interpretation of the Character of Electron Diffraction Patterns](#)

Am. J. Phys. **14**, 36 (1946); 10.1119/1.1990767

[Diffuse Electron Diffraction Patterns](#)

J. Chem. Phys. **6**, 749 (1938); 10.1063/1.1750164

---



# THE JOURNAL OF CHEMICAL PHYSICS

VOLUME 15, NUMBER 5

MAY, 1947

## The Interpretation of Electron Diffraction Patterns from Hydrocarbon Films\*

J. KARLE

*U. S. Naval Research Laboratory, Washington, D. C.*

AND

L. O. BROCKWAY

*University of Michigan, Ann Arbor, Michigan*

(Received January 7, 1947)

The theoretical expressions previously derived for the scattering of electrons by oriented hydrocarbon chains have been extended and applied to the calculation of characteristic diffraction patterns. These patterns are analyzed to form a basis for obtaining information about the molecular orientation. For the long chain molecules, the azimuthal direction, and the declination from the vertical may be determined independently. The orientation of the hydrocarbon chain about its own axis is less easily established, since it is determined only from the intensity distribution within the separate diffraction orders. When the declination is sufficiently large, randomness in the azimuthal directions is distinguished by the crossed-line pattern obtained. Randomness in the declination from the vertical may be estimated from the irregular spacing of the intercepts of the crossed lines. Quantitative intensity data would permit a more precise study of the angular distribution of the declination, and also of the orientation of the hydrocarbon chain about its own axis.

THE formation of films of close packed long-chain molecules on a water surface by the Langmuir technique has been known for some time, but the recent studies by Zisman *et al.*<sup>1</sup> of the oleophobic properties of films formed on solid surfaces by adsorption of long-chain molecules from dilute solutions have indicated the importance of adsorbed films in relation to

lubrication and corrosion inhibition problems. Since the unique properties of adsorbed films of long-chain molecules appear to be related to the molecular orientations in the films, it was considered valuable to pursue an investigation of the structure of these films with the aid of electron diffraction. Several types of diffraction patterns characteristic of hydrocarbon films have already been observed,<sup>2</sup> and the present paper considers the detailed analysis of typical photographs in terms of the orientation of the molecules, including the effects of randomness.

The theoretical scattering functions have been

\* This report concerns part of a study of films on metals authorized by the Chemistry Division of the Naval Research Laboratory under Contract No. N173s-10452 (June 15, 1945), and undertaken at the University of Michigan under the direction of the Department of Engineering Research, Project M639. The investigations included here were completed at the Naval Research Laboratory under Project No. N2002BR.

<sup>1</sup> W. C. Bigelow, D. L. Pickett, and W. A. Zisman, "Oleophobic Monolayers; Part I, Films Adsorbed from Solution in Non-Polar Liquids," *J. Colloid Sci.* **1**, 513 (1946); Part II, "Effect of Temperature on Adsorption," to be published.

<sup>2</sup> L. O. Brockway and J. Karle, "Electron Diffraction Study of Oleophobic Films on Copper, Iron and Aluminum," to be published in *J. Colloid Sci.*; L. O. Brockway and R. L. Livingston, "Electron Diffraction Study of Oleophobic Films on Platinum," to be published.

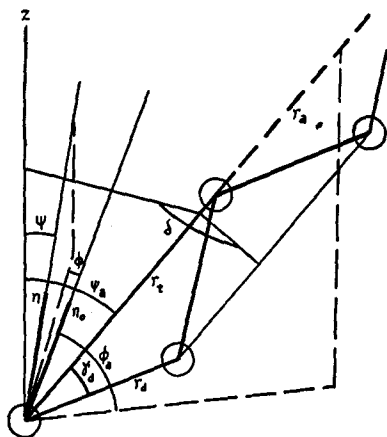


FIG. 1. The orientation of the hydrocarbon chain is determined by angles  $\psi_a$ ,  $\phi_a$ , and  $\delta$ . Also shown are the internal structural parameters  $r_t$ ,  $r_d$ , and  $\gamma_d$ , the main beam,  $\bar{n}_0$ , and the deviated beam,  $\bar{n}$ , with its polar coordinates  $\psi$  and  $\phi$ .

developed for several cases,<sup>3</sup> and they are used here in the calculation of intensity contour maps which show the appearance of patterns corresponding to several different orientations. The results and conclusions based on these maps are presented below.

### CALCULATION OF MAPS

The carbon atoms in the long-chain hydrocarbon molecules comprising an adsorbed film form a staggered chain and are assumed to be coplanar. There are therefore two parallel rows of carbon atoms in each chain. We may consider the row which contains the carbon atom closest to the surface as the axis of the molecule,  $\bar{r}_a$  (see Fig. 1).  $\psi_a$  is the angle defining the tilt of this axis from a normal to the surface of attachment,  $z$ , and  $\phi_a$  the angle of rotation of the  $\bar{r}_a z$  plane from the  $\bar{n}_0 z$  plane which is normal to the photographic plate. The angle,  $\delta$ , measures the rotation of the plane of the carbon atoms about axis  $\bar{r}_a$  from the  $\bar{r}_a z$  plane. The orientation of the hydrocarbon chain is completely described by angles  $\psi_a$ ,  $\phi_a$ , and  $\delta$ .

The internal structural parameters of the chain are  $r_t$ , the spacing of the carbon atoms along a row,  $r_d$ , the C—C bonded distance and  $\gamma_d$  the angle between them. Owing to the regularity of the structure of the carbon chain only two of these parameters are independent. The coordi-

nates of a point on the scattered beam,  $\bar{n}$ , are: (1)  $r$ , its radial extension into space; (2)  $\psi$ , the tilt of  $\bar{n}$  from the vertical axis,  $z$ ; and (3)  $\phi$ , the rotation of the  $\bar{n}z$  plane from the  $\bar{n}_0 z$  plane. The value of  $r$  is practically invariant over the area of a photographic plate ordinarily considered.

A formula for the intensity of electron scattering from a hydrocarbon chain must contain the orientation parameters ( $\psi_a$ ,  $\phi_a$ , and  $\delta$ ), the internal structural parameters ( $r_t$  and  $\gamma_d$ ), and the coordinates of a point on the scattered beam ( $\psi$ ,  $\phi$ , and  $r$ ). The formulae previously derived<sup>3</sup> concern various configurations of the carbon chains on the surface of attachment, that is to say special cases regarding the orientation parameters. The assumption was made in deriving the formulae that the electron scattering from the hydrogen atoms on the hydrocarbon chain is negligible. In addition the distribution of the molecules in the film was considered to be sufficiently irregular so that there arises no detectable inter-molecular interaction. In performing the calculations the value used for the bonded carbon to carbon distance in the chain was 1.54Å, and the bond angle was given the regular tetrahedral value. The number of atoms in the chain,  $N$ , was assumed equal to sixteen, the value of the wave-length of the electrons,  $\lambda$ , equal to 0.07Å, and the distance of the point of scattering from the origin of the photographic plate,  $L$ , equal to 35 cm. In the first four cases the angle of tilt of the molecular axis from the vertical to the surface was set equal to 20°, and in the fifth case it assumed random values. The formulae were expressed for convenience in terms of the cartesian coordinates  $x$  and  $y$  defined for a photographic plate by using relations (8) and (9) in reference (3). The point at which the main beam strikes is considered to be the origin,  $y$  is the axis parallel to the surface normal,  $z$ , and  $x$  is the axis parallel to the plane of the supporting surface. The intensity of electron scattering was calculated on an arbitrary scale for the contour maps and the first three orders were obtained.

The values of sines and cosines were obtained from *Tables of Sines and Cosines for Radian Arguments*, Federal Works Agency, Works Projects Administration, Project No. 765-97-3-10, New

<sup>3</sup> J. Karle, J. Chem. Phys. 14, 297 (1946).

York, 1940. The values of the Bessel functions were obtained from: (a) British Association for the Advancement of Science, Mathematical Tables, Volume VI Bessel Functions, Part I Functions of orders 0 and unity, University Press, Cambridge, 1931; (b) G. N. Watson, *Bessel Functions* (The Macmillan Company, New York, 1944), p. 730; (c) Gray, Mathews and MacRobert, *A Treatise on Bessel Functions* (The Macmillan Company, New York, 1931), p. 286.

### Case I

The molecules are fixed in space and, accordingly, angles  $\psi_a$ ,  $\phi_a$ , and  $\delta$  are given specific arbitrary values. The formula for this case is

$$\frac{f_e^2 \sin^2(Nsr_t \cos\alpha_a/4)}{r^2 \sin^2(sr_t \cos\alpha_a/2)} [1 + \cos(sr_d \cos\alpha_d)], \quad (1)$$

where

$$\cos\alpha_a = \cos\psi_n \cos\psi_a + \sin\psi_n \sin\psi_a \cos(\phi_a - \phi_n),$$

$$\begin{aligned} \cos\alpha_d &= \cos\alpha_a \cos\gamma_d + \sin\gamma_d \cos\beta \cos\delta \\ &\quad - \sin\gamma_d \sin\psi_n \sin(\phi_a - \phi_n) \sin\delta, \\ \cos\beta &= \cos\psi_n \sin\psi_a - \sin\psi_n \cos\psi_a \cos(\phi_a - \phi_n), \\ s &= 2\pi|\bar{n} - \bar{n}_0|/\lambda, f_e = (6 - F_e)/s^2, \end{aligned}$$

and  $N$ , the total number of carbon atoms in the chain, is necessarily even when using (1).  $\lambda$  is the electron wave-length dependent upon the voltage, and  $F_e$  is the scattering factor of carbon for x-rays, which is tabulated.<sup>4</sup> The angle  $\psi_n$  is the tilt of the  $\bar{n} - \bar{n}_0$  vector from the surface normal,  $z$ , and angle  $\phi_n$  measures the rotation of the  $(\bar{n} - \bar{n}_0)z$  plane from the  $\bar{n}_0z$  plane. The model chosen for Case I was given a rotation out of the  $\bar{n}_0z$  plane (angle  $\phi_a$ ) equal to  $45^\circ$ . The second row of carbon atoms was considered to hang down from axis  $\bar{r}_a$ , and therefore angle  $\delta$  was set equal to  $180^\circ$ . The result is shown in Fig. 2.

The distribution of intensity along the first and second orders was studied as a function of the rotation of the molecular plane in two auxiliary calculations. For a molecule with

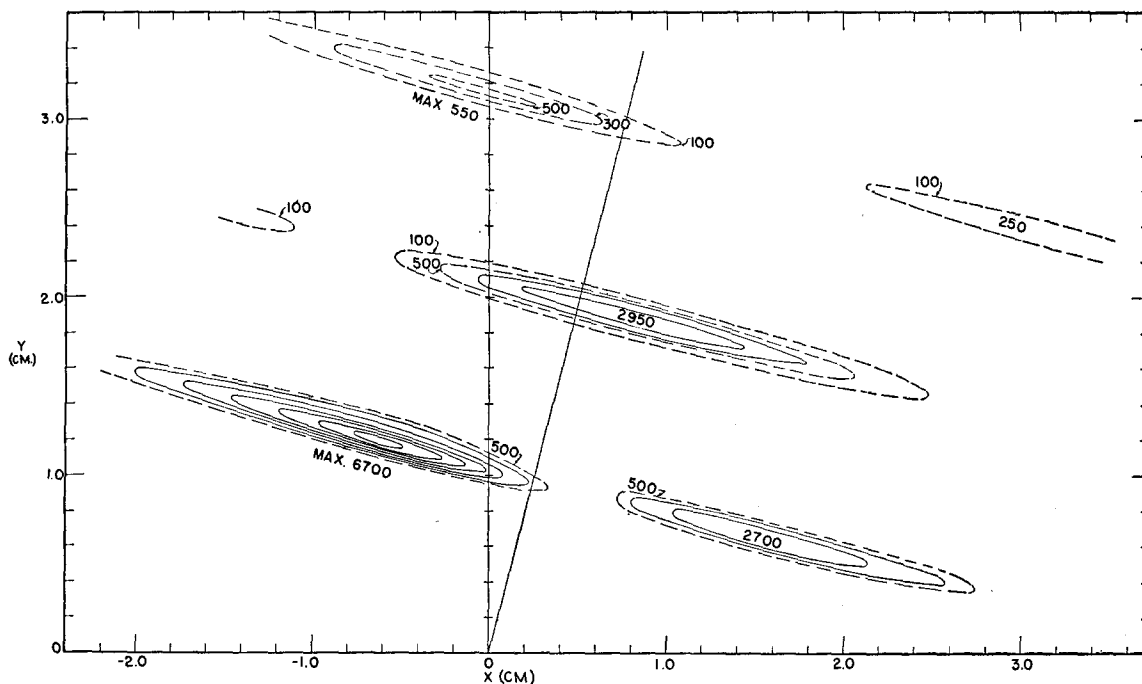


FIG. 2. Calculated pattern for Case I (formula 1). Angles  $\psi_a = 20^\circ$ ,  $\phi_a = 45^\circ$ , and  $\delta = 180^\circ$ . The solid contours are spaced by 1000 on the arbitrary scale. The line perpendicular to the successive orders is the projection of the molecular axis. The maxima of the intensity contours are indicated.

<sup>4</sup> *Internationale Tabellen Zur Bestimmung Von Kristallstrukturen* (J. W. Edwards, Ann Arbor, Michigan, 1944), revised edition, Vol. II, p. 571.

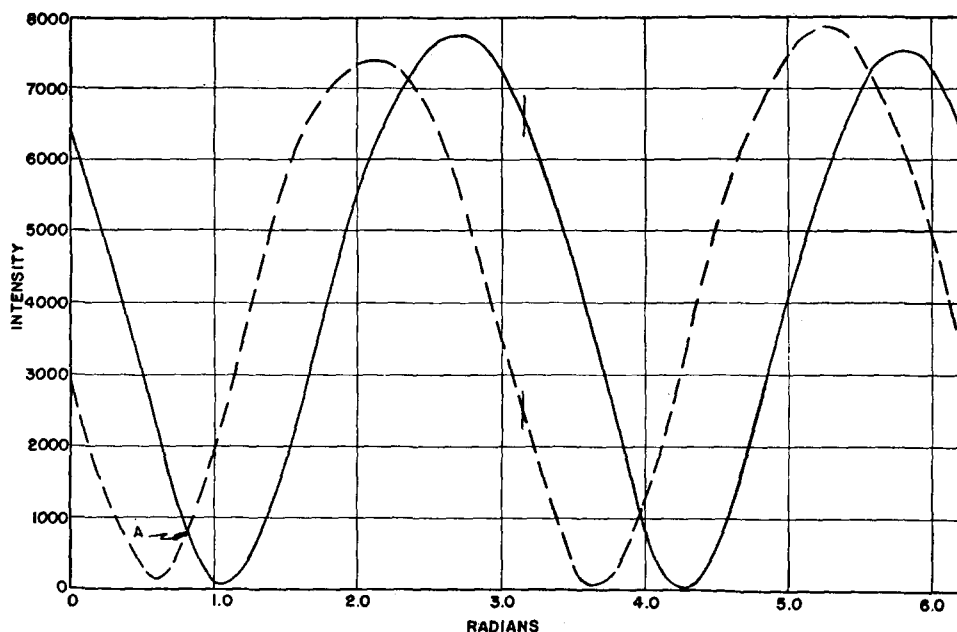


FIG. 3. Variation of intensity for two points placed symmetrically about projection of molecular axis in first order of Case I ( $\psi_a = 20^\circ$  and  $\phi_a = 45^\circ$ ) as  $\delta$  varies from 0 to  $2\pi$ . For solid line,  $x = -0.62$ ,  $y = 1.19$  and for dotted line,  $x = 1.12$  and  $y = 0.74$ . Point A corresponds to the value of  $\delta$  for which the plane of the hydrocarbon chain is perpendicular to the photographic plate. Vertical lines are placed at  $\delta = 180^\circ$ , the value in Fig. 2.

$\psi_a = 20^\circ$  and  $\phi_a = 45^\circ$  (as in Case I), the intensity was calculated at two points lying in the first order at equal distances from the projection of the molecular axis ( $x = -0.62$ ,  $y = 1.19$  and  $x = 1.12$ ,  $y = 0.74$ ). The intensity at these two points is plotted as a function of  $\delta$  in Fig. 3. Similar results for the second order ( $x = 0.30$ ,  $y = 1.97$ ;  $x = 0.70$ ,  $y = 1.87$ ) are shown in Fig. 4.

The effect of rotating the molecule about  $\bar{r}_a$  was also calculated for the special case of a vertical molecule. Distributions along the first and second orders were obtained for the plane of the carbon chain both parallel and perpendicular to the photographic plate. An additional calculation was made for the first order distribution when the plane of the chain is tilted  $45^\circ$  to the

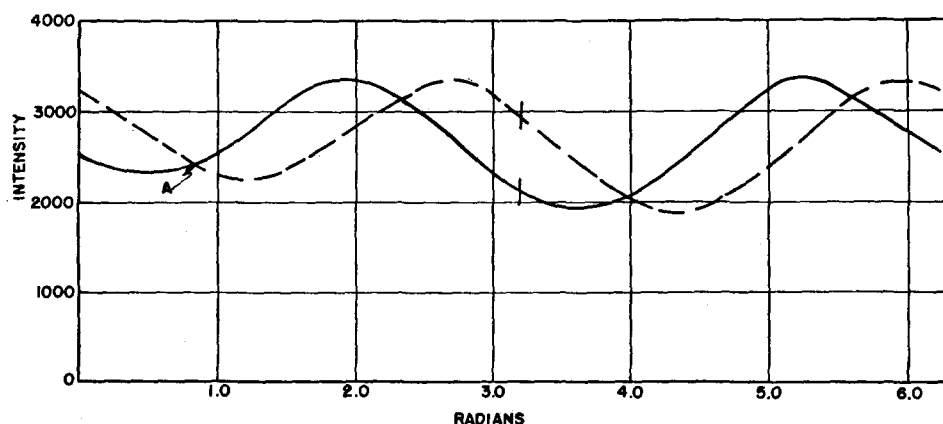
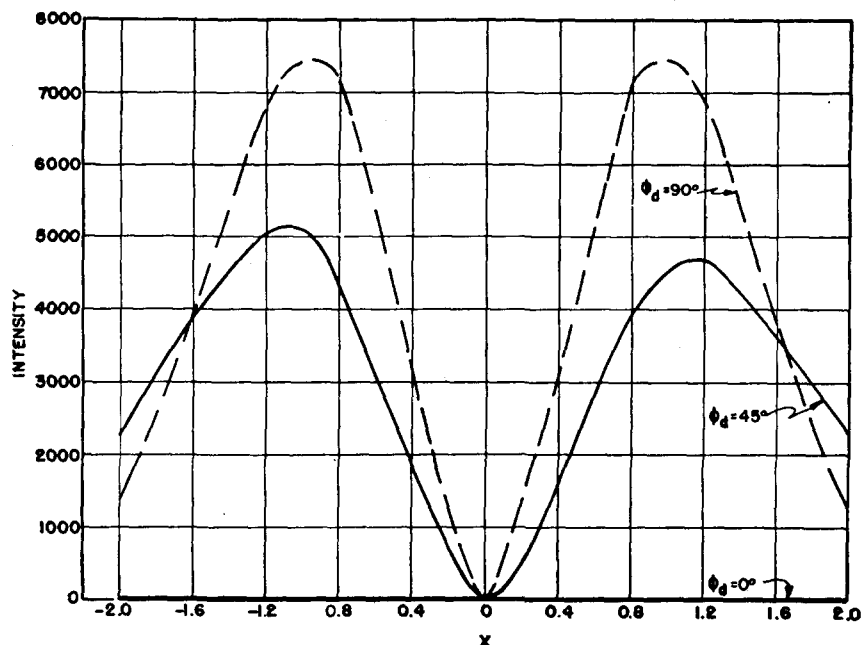


FIG. 4. Variation of intensity for two points placed symmetrically about projection of molecular axis in second order of Case I ( $\psi_a = 20^\circ$  and  $\phi_a = 45^\circ$ ) as  $\delta$  varies from 0 to  $2\pi$ . For solid line,  $x = 0.30$ ,  $y = 1.97$  and for dotted line  $x = 0.70$ ,  $y = 1.87$ . Point A and the vertical markers have the same significance as in Fig. 3.

FIG. 5. Variation of intensity in first order for molecule with axis vertical and the indicated values for the orientation of the plane of the carbon chain (see text concerning  $\phi_d$ ).



photographic plate. The formula used is

$$\frac{f_o^2 \sin^2(Nsr_i \cos\psi_n/4)}{r^2 \sin^2(sr_i \cos\psi_n/2)} \times [1 + \cos(r_{ds} \cos\psi_n \cos\gamma_d + r_{ds} \sin\psi_n \sin\gamma_d \cos(\phi_n - \phi_d))], \quad (2)$$

where  $\phi_d$  measures the rotation of the plane of the molecule from the  $\bar{n}_0z$  plane. (Angle  $\phi_d$  determines the orientation of the plane of the chain for a vertical molecule just as angle  $\delta$  serves for the general case. It is necessary though

to distinguish between the two since they are not similarly defined.) In performing the calculation, the value of  $y$  for which the ratio of the sine squared terms is a maximum was determined, and then the values of the function were calculated for varying values of  $x$  and the latter value of  $y$ . For the calculations in this article, the values  $0^\circ$ ,  $45^\circ$  and  $90^\circ$  were chosen for angle  $\phi_d$ . The results are shown in Figs. 5 and 6.

## Case II

The axes of the molecules in a film are fixed in space, and the planes of the carbon chains

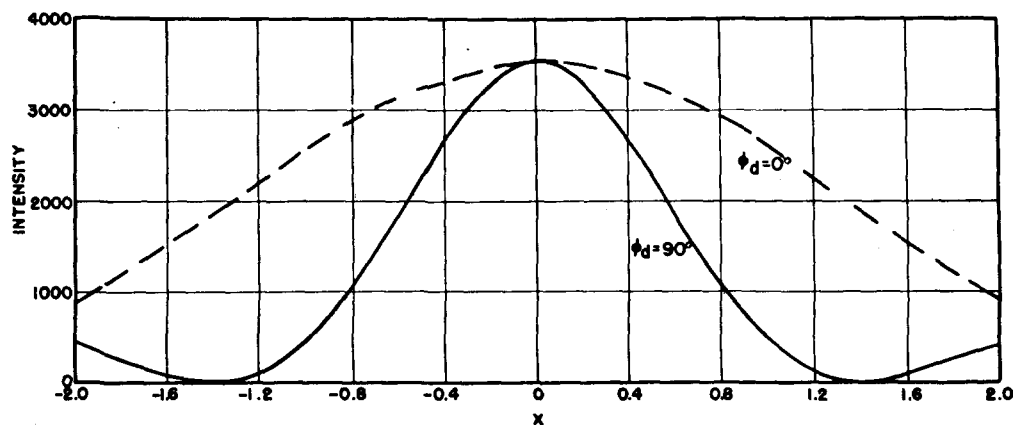


FIG. 6. Variation of intensity in second order for molecule with axis vertical and the indicated values for the orientation of the plane of the carbon chain.

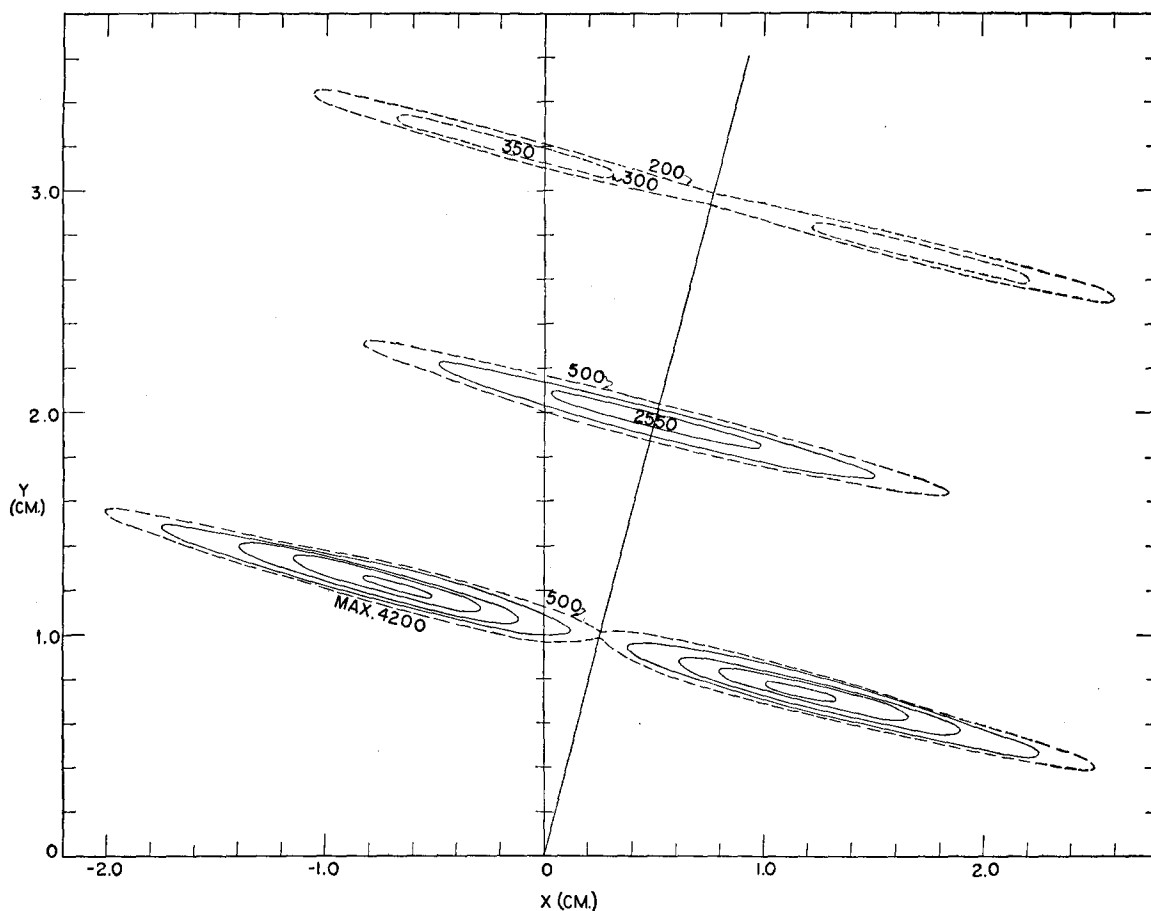


FIG. 7. Calculated pattern for Case II (formula 3). Angles  $\psi_a = 20^\circ$ ,  $\phi_a = 45^\circ$ , and  $\delta$  is random. The solid contours are spaced by 1000 on the arbitrary scale. The projection of the molecular axis and the maxima of the intensity contours are indicated.

assume random positions about these axes. The formula used is:

$$\frac{f_c^2 \sin^2(Nsr_t \cos \alpha_a/4)}{r^2 \sin^2(sr_t \cos \alpha_a/2)} \times [1 + \cos(sr_d \cos \gamma_d \cos \alpha_a) \times J_0(sr_d \sin \gamma_d \sin \alpha_a)], \quad (3)$$

where  $J_0$  is the Bessel function of zero order. The other quantities have been defined above. This calculation is different from the first one only insofar as the contribution from all possible values of  $\delta$  is considered. The result is shown in Fig. 7.

### Case III

The tilt of the molecular axes and the orientation of the planes of the carbon chains are

arbitrarily specified. The molecules, however, assume random positions about the surface normal,  $z$ . The formula used is

$$\begin{aligned} & \frac{Nf_c^2}{2r^2} + \frac{f_c^2}{r^2} \sum_{\nu=1}^{(N-2)/2} 2\nu \cos[(N/2 - \nu)A] \\ & \times J_0[(N/2 - \nu)B] \\ & + \frac{f_c^2}{r^2} \sum_{\mu=1}^{N/2} \mu \cos[(N+1)/2 - \mu)A + C] \\ & \times J_0[(N+1)/2 - \mu)B - D)^2 + E^2]^{\frac{1}{2}} \\ & + \frac{f_c^2}{r^2} \sum_{\lambda=1}^{(N-2)/2} \lambda \cos[-(N-1)/2 - \lambda)A + C] \\ & \times J_0[(N-1)/2 - \lambda)B - D)^2 + E^2]^{\frac{1}{2}}, \quad (4) \end{aligned}$$

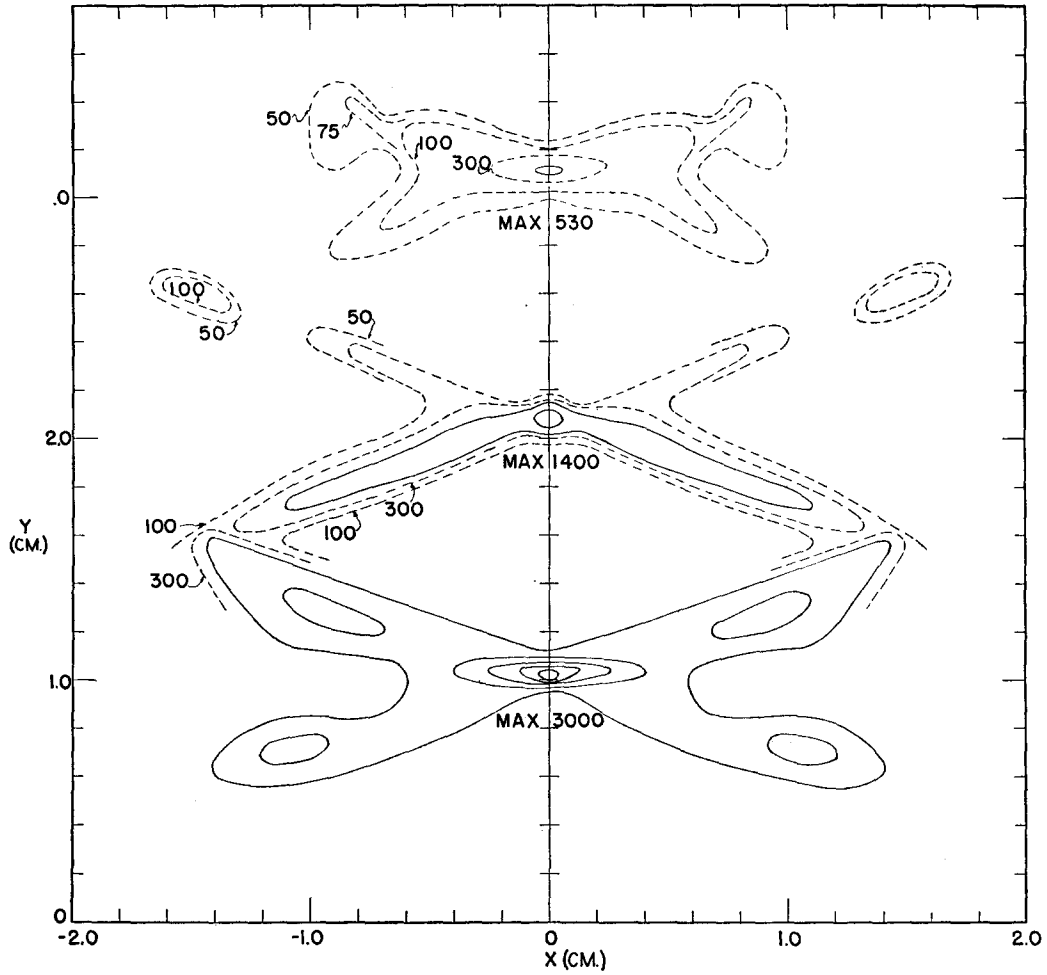


FIG. 8. Calculated pattern for Case III (formula 4). Angles  $\psi_a = 20^\circ$ ,  $\delta = 180^\circ$ , and angle  $\phi_a$  is random. The solid contours are spaced by 500.

where

$$\begin{aligned} A &= r_t \cos \psi_{as} \cos \psi_n, \\ B &= r_t \sin \psi_{as} \sin \psi_n, \\ C &= r_0 \sin \psi_{as} \cos \psi_n \cos \delta, \\ D &= r_0 \cos \psi_{as} \sin \psi_n \cos \delta, \\ E &= r_0 s \sin \psi_n \sin \delta. \end{aligned}$$

This calculation differs from the first one in that the contribution from all possible values of  $\phi_a$  is considered. The result is shown in Fig. 8.

#### Case IV

The tilt of the axes of the molecules is arbitrarily specified. The molecules are randomly distributed about the surface normal,  $z$ , and also about their own axes. The formula used is

$$\begin{aligned} & \frac{N f_c^2}{2 r^2} + \frac{f_c^2 (N-2)^{1/2}}{r^2} \sum_{\nu=1}^{\infty} 2\nu \cos[(N/2 - \nu)A] \\ & \quad \times J_0[(N/2 - \nu)B] \\ & + \frac{f_c^2 N^{1/2}}{\mu^2} \sum_{\mu=1}^{\infty} (2\mu - 1) \cos[(N+1]/2 - \mu)A] \\ & \quad \times \sum_{m=0}^{\infty} (-1)^m \epsilon_m J_{2m}(sr_0 a) J_{2m}(sr_0 b) \\ & \quad \times J_{2m}[(N+1]/2 - \mu)B] \\ & + \frac{f_c^2 N^{1/2}}{r^2} \sum_{\mu=1}^{\infty} (2\mu - 1) \sin[(N+1]/2 - \mu)A] \\ & \quad \times \sum_{m=0}^{\infty} (-1)^{m+1} 2 J_{2m+1}(sr_0 a) \\ & \quad \times J_{2m+1}(sr_0 b) J_{2m+1}[(N+1]/2 - \mu)B], \quad (5) \end{aligned}$$



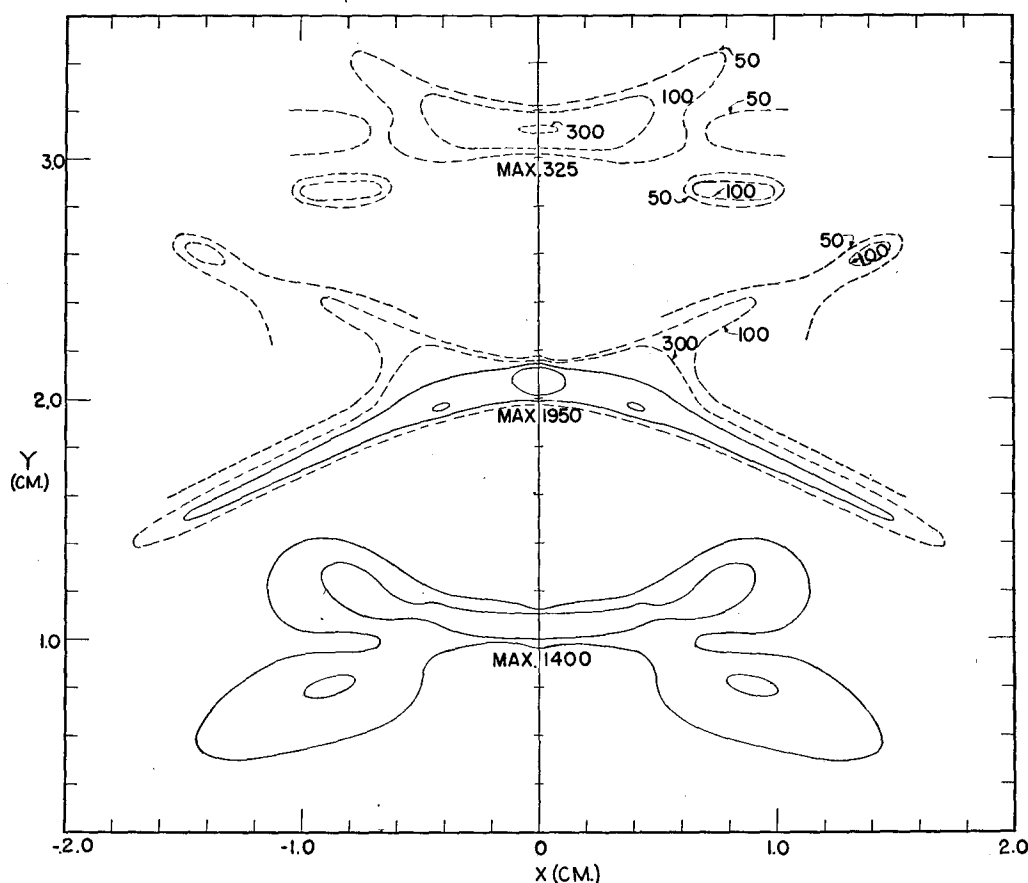


FIG. 9. Calculated pattern for Case IV (formula 5). Angle  $\psi_a = 20^\circ$ , and angles  $\phi_a$  and  $\delta$  are random. The solid contours are spaced by 500.

where

$$\begin{aligned} a^2 &= [P + (P^2 - Q^2)^{1/2}] / 2, \\ b^2 &= Q^2 / [2P + 2(P^2 - Q^2)^{1/2}], \\ P &= 1 - \cos^2 \psi_n \cos^2 \psi_a, \\ Q &= 2 \cos \psi_n \cos \psi_a \sin \psi_n \sin \psi_a, \end{aligned}$$

$\epsilon_m = 1$  when  $m = 0$ ,  $\epsilon_m = 2$  when  $m \neq 0$ , and  $J_n$  is the Bessel function of order  $n$ . This calculation differs from the second one in that the contribution from all possible values of  $\phi_a$  is considered. The result is shown in Fig. 9.

### Case V

The first four calculations given in detail in reference (3) were based on various orientations in which the tilt of the molecular axis remained fixed. The effect of a variation in angle  $\psi_a$  on

the position of the  $y$ -intercept of successive orders was of particular interest since it was observed that the spacings varied in some photographs. This variation was introduced into formula (4) of Case III by inserting approximations which are valid in the vicinity of the  $y$  axis and then averaging over all values of  $\psi_a$ , from 0 to  $20^\circ$  using the assumption that all values of  $\psi_a$  in this range are equally probable. The calculation was restricted to points along the  $y$  axis including the first four orders.

As in Case III angle  $\delta$  was set equal to  $180^\circ$ ,  $N = 16$ ,  $\lambda = 0.07\text{A}$ , and  $L = 35\text{ cm}$ . In addition the  $J_0$  were set equal to unity since  $\sin \psi_n$  is almost zero for the region of the  $y$  axis under consideration. We may write  $\cos \psi_a - 1 = \psi_a^2 / 2$ , and  $\sin \psi_a = \psi_a$  in formula (4) and then average this expression over  $\psi_a$  from 0 to  $20^\circ$ . The result is

$$\begin{aligned}
& \frac{8f_c^2}{r^2} + \frac{f_c^2}{r^2} \sum_{\nu=1}^7 \frac{2\nu}{G} \left( \cos H \int_0^G \cos \phi^2 d\phi \right. \\
& \quad \left. + \sin H \int_0^G \sin \phi^2 d\phi \right) \\
& + \frac{f_c^2}{r^2} \sum_{\mu=1}^8 \frac{\mu}{J} \left( \cos[K+L] \int_{L^{\frac{1}{2}}}^{J+L^{\frac{1}{2}}} \cos \phi^2 d\phi \right. \\
& \quad \left. + \sin[K+L] \int_{L^{\frac{1}{2}}}^{J+L^{\frac{1}{2}}} \sin \phi^2 d\phi \right) \\
& + \frac{f_c^2}{r^2} \sum_{\omega=1}^7 \frac{\omega}{M} \left( \cos[N+P] \int_{-P^{\frac{1}{2}}}^{M-P^{\frac{1}{2}}} \cos \phi^2 d\phi \right. \\
& \quad \left. + \sin[N+P] \int_{-P^{\frac{1}{2}}}^{M-P^{\frac{1}{2}}} \sin \phi^2 d\phi \right), \quad (6)
\end{aligned}$$

where

$$\begin{aligned}
G &= \pi(H/2)^{\frac{1}{2}}/9, \\
H &= (8-\nu)r_t s \cos \psi_n, \\
J &= \pi(K/2)^{\frac{1}{2}}/9, \\
K &= (8.5-\mu)r_t s \cos \psi_n, \\
L &= (r_0 s \cos \psi_n)^2/2K, \\
M &= \pi(N/2)^{\frac{1}{2}}/9, \\
N &= (7.5-\omega)r_t s \cos \psi_n, \\
P &= (r_0 s \cos \psi_n)^2/2N.
\end{aligned}$$

The integrals involved were calculated from the related Fresnel integrals.<sup>5</sup> The result is shown in Fig. 10.

### DISCUSSION OF CONTOUR MAPS

The contour diagrams of the intensities, all plotted on the same arbitrary scale, are shown in Figs. 2, 7, 8 and 9. The pattern in Fig. 2 from an oriented molecule shows the expected concentration of scattered electrons along a series of parallel lines normal to the projection of the molecular axis. The intensity distribution in the successive orders is characteristic of the double row of atoms in which the second is displaced relative to the first by half the identity distance along the row. The pattern from a single row of carbon atoms would show parallel lines in the same positions, but with intensity decreasing with increasing distance from the main beam, as required by the atomic scattering factor. The odd orders in Fig. 2 show a minimum near the projection of the molecular axis, and the even orders show a maximum, but the value chosen for the angle  $\delta$  causes these minima and maxima to lie off the axis, with a generally asymmetric intensity distribution. In the first order the intensity on the left of the axis reaches a value about twice as great as that on the right.

In Fig. 7 calculated for random values of  $\delta$ , the intensity pattern is symmetric about the projection of the molecular axis. It is therefore clear that as the value of  $\delta$  changes, the intensity distribution along the layer lines varies. This is depicted in Figs. 3 and 4. It is seen that the

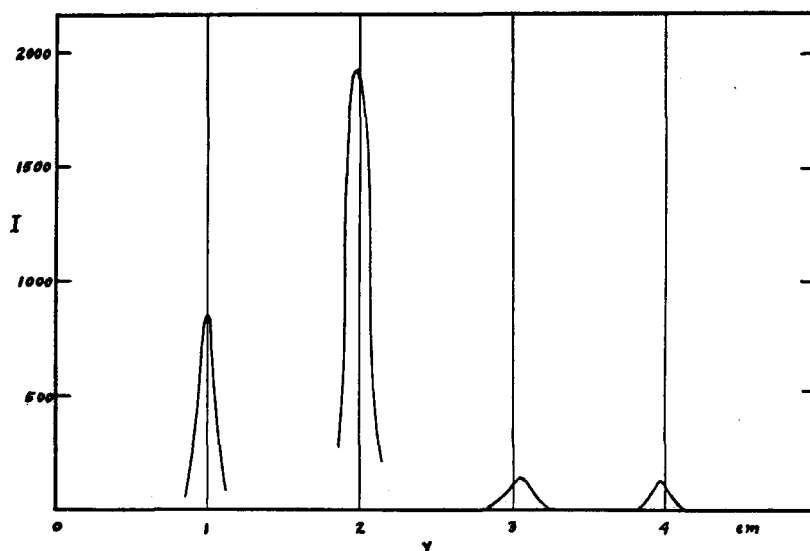


FIG. 10. Calculated pattern for Case V (formula 6). The variation of the intensity is shown along the  $y$  axis in the vicinity of the maxima of the first four orders. Angle  $\delta = 180^\circ$ ,  $\phi_a$  is random, and  $\psi_a$  varies from  $0^\circ$  to  $20^\circ$ .

<sup>5</sup> British Association for the Advancement of Science, *Calculation of Mathematical Tables*, 273 (1926).

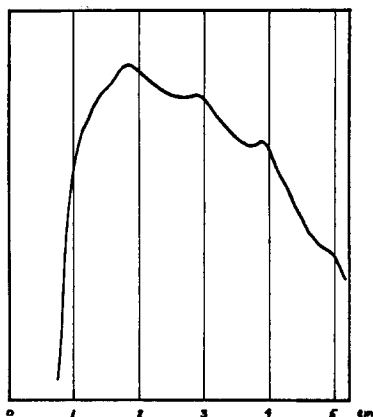


FIG. 11. Microphotometer trace of Fig. 12 along  $y$  axis showing difference in spacing between second and third, and third and fourth maxima. Position of main beam is altered by refraction.

variations in the first order are larger than those in the second order, and that the intensities at points symmetrically placed with respect to the projection of the molecular axis have the same range of values, but not in phase. This accounts for the asymmetry of the resulting patterns for particular values for the angle  $\delta$ . A change by  $\pi$  radians in  $\delta$  has little effect on the intensity. The intersection of low intensities, point  $A$ , in Fig. 3 corresponds to a value of  $\delta$ , which makes the plane of the carbon chain perpendicular to the photographic plate.

The great variations of the intensity of the first order and the smaller variations in the second order with changes in angle  $\phi_a$  are shown for a molecule with its axis vertical in Figs. 5 and 6. The intensity in the first order is lowest when the plane of the chain is perpendicular to the photographic plate and greatest when the chain is parallel. The asymmetry in the patterns for different positions of the plane of the chain about the molecular axis is very small when the axis is vertical. The greater asymmetry shown by Figs. 3 and 4 is associated with the  $20^\circ$  tilt of the molecular axis.

The effect on scattering from molecules assuming random positions about the surface normal instead of maintaining a fixed position may be seen by comparing Fig 8 to Fig. 2. Fig. 9. is similarly related to Fig. 7. In all these cases the tilt of the molecular axes is  $20^\circ$ . Figures 8 and 9 may be described roughly as crossed-line pat-

terns. The position of the maxima on the  $y$  axis are evenly spaced and have the same intensity and position as those in Figs. 2 and 7, respectively. This was anticipated since it was pointed out previously<sup>3</sup> that in the region of the photographic plate ordinarily considered, the intensity along the  $y$  axis is virtually independent of angle  $\phi_a$ . Figure 9 differs from Fig. 8 in that the second row of carbon atoms assumes random positions about the molecular axis. In both cases the first and third orders are spread out, that is, the intensity changes gradually and hence would appear weak to the eye. The second order shows a sharp change of slope and would appear dark. It should be noted that the tilt of these orders from a horizontal axis is about  $14^\circ$  and not  $20^\circ$ , the value of  $\psi_a$ . The major difference in Figs. 8 and 9 is the intensity of the maxima along the  $y$  axis.

The qualitative appearance of these maps may be compared with Fig. 12, a diffraction pattern from an oleophobic film formed on rolled platinum from a 0.05 percent cerotic acid solution in cetane. The first order that appears on the print is actually the second order. Although Fig. 12 has many of the characteristics of Figs. 8 and 9, it is apparent that the maxima along the  $y$  axis are not evenly spaced. This is borne out by the microphotometer trace in Fig. 11. It was proposed that since the maxima along the  $y$  axis are mainly determined by the angle of tilt of the molecular axis, uneven spacings may be caused by a randomness in this tilt. Calculation V was therefore performed to show the effect of this variation, and the resultant intensities along the  $y$  axis are plotted in Fig. 10. It is noted that the spacing between the second and third orders is 17 percent greater than that between the third and fourth orders, while in the photometer trace, Fig. 11, the spacing is 15 percent greater. It will be recalled that the assumption made in calculating Fig. 10 was equal probability for all positions between  $0^\circ$  and  $20^\circ$ . Analysis of Fig. 12 indicates that angle  $\psi_a$  assumes values as large as  $30^\circ$ . It is possible that the distribution leading to Fig. 12 resembles more closely that on the surface of a sphere, in which case the population would be proportional to  $\sin\psi_a$ . This type of distribution would make the contribution from the larger tilts more im-

portant and reduce the magnitude of the difference in spacings of successive orders.

### INTERPRETATION OF PATTERNS

The question arises concerning what conclusions may be drawn from the analysis of the diffraction patterns of a hydrocarbon film, in view of the calculations performed above. In effect, we are concerned with determining the values of  $\psi_a$ ,  $\phi_a$ , and  $\delta$  for the many molecules comprising a film. To a certain extent independent effects from these angles are obtained in the scattering patterns which allow separate evaluations of each of these orientation parameters.

The value of angle  $\psi_a$  may be determined from the positions of the intercepts of successive orders on the  $y$  axis. When angle  $\psi_a$  has a fixed value among the many molecules comprising a film, the intercepts are very nearly evenly spaced, and their separations may be expressed in terms of the carbon to carbon distance along a single row of atoms,  $r_t$ , as follows:

$$y = nL\lambda / r_t \cos\psi_a, \quad (7)$$

where  $n$  refers to the order. This expression has been used previously to determine the tilt of the axes of long chain molecules by Germer and Storks.<sup>6</sup> When angle  $\psi_a$  assumes a range of values the spacings of the intercepts of successive orders on the  $y$  axis do not remain constant (see Fig. 10). This result cannot be derived from expression (7). It arises from considering the scattered intensity of the entire staggered carbon chain instead of that from a single row of atoms.

For the purpose of making quantitative estimates, an average value for angle  $\psi_a$  may be obtained from expression (7) by measuring the spacings between the second and fourth orders. These latter orders are affected similarly, and to about the same extent, by variations in angle  $\psi_a$ . The spread about this average value can be approximated from the difference in spacing between the second and third, and the third and fourth orders. Some estimate of the magnitude of the spread may be based on the results obtained in Figs. 10 and 11. It should be borne in mind that the quantitative conclusions so drawn are necessarily quite rough if the investigator does not know the weight function to be applied to the angular distribution. Variations in the value of angle  $\delta$  will have a small additional effect on the relative spacings. It should be noted that the foregoing remarks concerning angle  $\psi_a$  apply irrespective of whether angle  $\phi_a$  varies or not, since, as was previously pointed out, the position and intensity of the intercepts on the  $y$  axis are independent of angle  $\phi_a$  for the region of the photographic plate ordinarily considered.

Methods of estimating the value of angle  $\phi_a$  may now be considered. If  $\phi_a$  has a fixed value, the scattering pattern shows a succession of orders perpendicular to the projection of the molecular axis (Figs. 2 and 7). The value of angle  $\phi_a$  may be obtained from the expression,

$$\frac{1}{\tan\psi_a \sin\phi_a}, \quad (8)$$

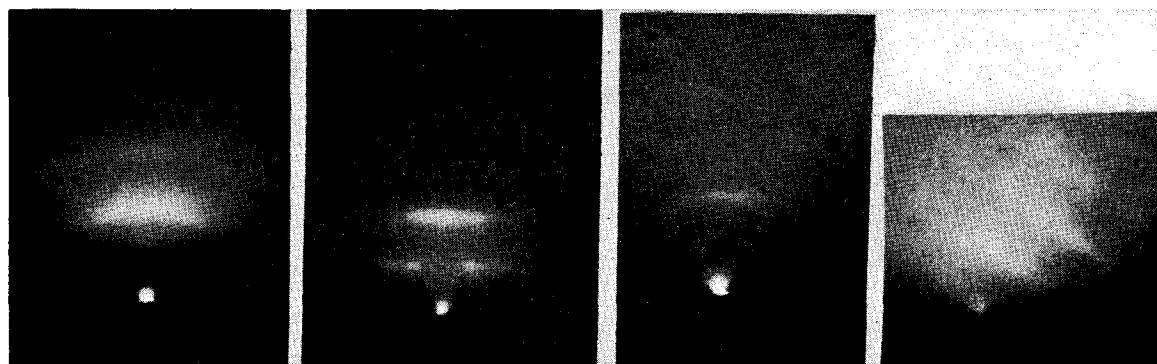


FIG. 12. Pattern from film of cerotic acid on flamed, rolled platinum foil.

FIG. 13. Pattern from film of cerotic acid on metallographically polished platinum.

FIG. 14. Pattern from film of stearic acid on cold rolled steel.

FIG. 15. Pattern from excess stearic acid crystallized on platinum foil.

<sup>6</sup> L. H. Germer and K. H. Storks, J. Chem. Phys. 6, 280 (1938).

which is the slope of the projection of the molecular axis on the photographic plate. This expression was used by Germer and Storks.<sup>6</sup> When angle  $\phi_a$  assumes all possible values from 0 to  $2\pi$  the pattern obtained is symmetric about the  $y$  axis. Random values of  $\phi_a$ , when  $\psi_a$  is large, produce patterns similar to Figs. 8 and 9. When  $\psi_a$  is small and  $\phi_a$  is random, the pattern is similar to the well-known patterns<sup>7</sup> of vertical molecules with random values of angle  $\phi_a$ . Angle  $\phi_a$  has no significance when angle  $\psi_a$  is zero.

For an estimation of the values of angle  $\delta$ , Figs. 3, 4, 5, and 6, are very helpful as a guide. They show that if angles  $\psi_a$  and  $\phi_a$  are fixed, the value of angle  $\delta$  will determine not only the relative intensities of the odd and even orders, but also the symmetry within a particular order. When  $\psi_a$  is small (less than  $10^\circ$ ) asymmetry effects are very small. When  $\psi_a$  is fixed and  $\delta$  is random, the pattern obtained will be symmetric about the projection of the molecular axis irrespective of the value of angle  $\phi_a$ . This symmetry does not occur for most fixed values of  $\delta$  and may be checked experimentally by varying angle  $\phi_a$ , which is accomplished by rotating the sample about a vertical axis,  $z$ . From noting the pattern asymmetry and knowing the values of angles  $\psi_a$  and  $\phi_a$ , and inserting them into formula (1), the value of angle  $\delta$  may be estimated. When angle  $\phi_a$  is random and  $\psi_a$  is large, the question of whether  $\delta$  is random or fixed is indicated from measuring the relative intensities of successive orders along the  $y$  axis. The differences which may occur are shown in Figs. 8 and 9. Additional calculations using formula (4) would need to be made to ascertain the values of the maxima along the  $y$  axis for various values of angle  $\delta$ . When  $\psi_a$  is small and  $\phi_a$  random, it is not possible to decide on the value of  $\delta$ . From the calculations performed so far it is also not possible to decide on the value of  $\delta$  generally when angle  $\psi_a$  assumes a range of values.

It is clear that many conclusions depend upon estimates of relative intensities. Visual estimates are quite poor, but microphotometer traces used in conjunction with the rotating-sector technique should aid considerably in estimating the intensities. The effects of incoherent scattering<sup>8</sup>

should be included in these considerations. The neglect of the scattering from hydrogen atoms in performing the calculations will have some effect on the intensities within the orders. This should not affect the validity of the analysis, though, since the hydrogen atoms have the same vertical identity spacing as the carbon atoms and hence will not affect the positions or the general shapes of the successive orders of scattering. Intermolecular interaction, that is scattering due to a regularly close-packed assemblage, may also affect the intensities within the orders. This effect will be quite negligible in films of randomly oriented molecules. When the molecules have a fixed orientation and regular spacing, the contribution from the distances between the molecules is readily recognized as spots along the order lines (see Fig. 13).

#### ILLUSTRATION OF METHOD

Several types of observed diffraction patterns are illustrated in Figs. 12, 13, 14, and 15. As indicated above, the crossed line pattern in Fig. 12 arises from molecules showing random values of  $\phi_a$ , with  $\psi_a$  ranging from  $0^\circ$  up to about  $30^\circ$ . This estimate is based on the observation that the average tilt of the molecular axis calculated from formula (7) from the spacing between the second and fourth maxima is  $16^\circ$ , and that the tilt of the successive orders on the pattern from a horizontal axis is about  $20^\circ$ . The range of orientation of the molecules giving rise to this photograph does not fix by itself the nature of the attachment of the molecule to the supporting surface. The random values for  $\psi_a$  would be accounted for in the specimen either by a variation in the angles between the molecules and the surface, or by a variation in the surface contour with all molecules fixed at this same angle at the point of attachment. Such questions have to be considered in the light of photographs taken from similar specimens using different methods of preparation. An illustration of this point is found in Fig. 13.

The pattern of horizontal lines observed in Fig. 13 indicates that the molecules are standing vertically. The effect of wide spacings between different molecules is manifested to a small degree in the intensity distribution along the first-order line. This pattern was also obtained

<sup>7</sup> C. A. Murison, *Phil. Mag.* **17**, 201 (1934).

<sup>8</sup> L. Bewilogua, *Physik. Zeits.* **32**, 740 (1931).

from cerotic acid, but on a surface which was smoothed by polishing, in contrast with the rolled surface used in Fig. 12. The differences between the molecular orientations exhibited in these two figures is associated with the difference in the method of preparing the platinum surface.

Figure 14 shows a pattern of stearic acid on iron in which the deviation from the vertical ranges over not more than  $10^\circ$ , while the values of  $\phi_a$  are random. An average value of  $5^\circ$  was obtained for  $\psi_a$  by measuring the spacing between the second and fourth maxima and using formula (7). The upper limit of  $10^\circ$  was set by assuming that the average value represents the mean of a variation starting at zero degrees. This assumption is supported by the fact that the spacing between the second and third orders is about six percent larger than the spacing between third and fourth. A microphotometer trace was found to be quite useful in corroborating the visual measurements.

Figure 15 shows a pattern of tilted layer lines obtained from stearic acid crystallized on platinum. This pattern arises from molecules having constant values of  $\phi_a$  and  $\psi_a$ , equal to  $64^\circ$  (or  $116^\circ$ ) and  $40^\circ$ , respectively, determined from using formulas (7) and (8). The intensity

distributions within the successive orders are not too clearly defined, but appear on the original negative to be symmetric with respect to a line perpendicular to them and intersecting the main beam. The odd orders are strongest on either side of this line, and the even orders are strongest at the intersections. Angle  $\delta$ , therefore, probably assumes random values. As pointed out above, this can be established by taking additional photographs at various values of  $\phi_a$  by rotating the specimen. Patterns with fixed orientation such as Fig. 15 were not observed so far for films believed to be monolayers.

The information of the kind obtained from the illustrations above has been of considerable assistance in studying the properties of oriented monolayers, and it is hoped that the information obtainable in some cases from electron diffraction photographs will advance the study of the physical and chemical properties of long chain organic molecules, especially in the adsorbed state.

#### ACKNOWLEDGMENT

The close interest of Dr. W. A. Zisman of the Naval Research Laboratory and the assistance of Dr. Isabella Karle are gratefully acknowledged.

### The Entropy of Solution of Molecules of Different Size

J. H. HILDEBRAND

*Department of Chemistry, University of California, Berkeley, California*

(Received February 25, 1947)

The entropy of mixing two liquids whose molecules differ in size is expressed in terms which avoid the assumption of a lattice as an artificial frame of reference, and which is not limited to linear polymers. The equation obtained is

$$\frac{\Delta S}{R} = N_1 \ln \frac{V - N_1 b_1 - N_2 b_2}{N_1(v_1 - b_1)} + N_2 \ln \frac{V - N_1 b_1 - N_2 b_2}{N_2(v_2 - b_2)},$$

where  $N_1$  and  $N_2$  denote number of moles,  $V$  the volume of the solution,  $v_1$  and  $v_2$  the molal volumes of the pure components and  $b_1$  and  $b_2$  the sum of the actual geometrical volumes of  $6 \times 10^{23}$  molecules. With certain simplifying assumptions, equivalent to those used by authors who have analyzed the problem for linear polymers in a lattice frame of reference, the above equation reduces to the form obtained by the latter method. Various methods of obtaining experimental values for  $b$  are outlined.

THE thermodynamic properties of solutions of long, linear molecules in the ordinary solvents have recently attracted considerable

attention by reason both of the commercial importance of high polymers and of the interesting problems in the entropy of mixing which their